Downscaling Fourier Transform Infrared Spectroscopy to the Micrometer and Nanogram Scale: Secondary Structure of Serotonin and Acetylcholine Receptors†

Per Rigler, Wolf-Peter Ulrich, Ruud Hovius, Erwin Ilegems, Horst Pick, and Horst Vogel*

Laboratoire de Chimie Physique des Polymères et Membranes, Ecole Polytechnique Fédérale de Lausanne, CH-1015 Ecublens, Switzerland

Received June 27, 2003; Revised Manuscript Received September 18, 2003

ABSTRACT: High signal-to-noise Fourier transform infrared (FTIR) spectra of the 5-hydroxytryptamine (serotonin) receptor (5-HT_3R) and the nicotinic acetylcholine receptor (nAChR) were obtained by microscope FTIR spectroscopy using micrometer-sized, fully hydrated protein films. Because this novel procedure requires only nanogram quantities of membrane proteins, which is 4−5 orders of magnitude less than the amount of protein typically used for conventional FTIR spectroscopy, it opens the possibility to access the structure and dynamics of many important mammalian receptor proteins. The secondary structure of detergent-solubilized 5-HT_3R determined by curve fitting of the amide I band yielded 36% α-helix, 33% β-strand, 15% β-turn, and 16% nonregular structures, which remained unchanged upon reconstitution in lipid membranes. From hydrogen−deuterium exchange, the secondary structure of the water-accessible part of 5-HT_3R was determined as 14% α-helix, 16% β-strand, 26% β-turn, and 14% nonregular structures. Interestingly, we found that both the overall and the water-accessible nAChR secondary structures were nearly identical to those of 5-HT_3R, in agreement with predicted structures of this class of receptors. This is the first time that structural investigations were obtained for two closely related ligand-gated ion channels under strictly identical experimental conditions.

Membrane proteins represent one-third of the human proteome. They fulfill central biological functions such as intra- and intercellular transport, nerve conduction, or cellular signaling, to mention a few (*1*). In consequence, they are important targets for therapeutic compounds. According to a recent survey, the majority of presently used and future novel medicines target membrane proteins, primarily ionotropic and G protein-coupled receptors (*2*). Despite substantial efforts, structures of only a few membrane proteins have been solved to atomic resolution, in contrast to many thousands of water-soluble proteins (*3*).

Major hurdles for this limited success in structural membrane biology are (i) the lack of purified, functional mammalian membrane proteins in sufficient amounts required for NMR spectroscopy (*4*) or for X-ray diffraction (*5*, *6*) or (ii) the resistance of most membrane proteins to crystallization. Therefore, efforts are made to use other biophysical techniques that require no crystals and less material but deliver information on structure, dynamics, and function of the membrane protein of interest. An outstanding example in this context is the work performed primarily by Ron Kaback's group to solve the structure and function of lactose permease, a prototypic transport protein (*7*). A high-resolution structure of this protein was recently obtained, confirming many structural predictions deduced from the above-mentioned indirect methods (*8*). In particular, Raman and infrared spectroscopy delivered important details on the structure and dynamics of membrane proteins (*9*−*11*).

A few examples underline the importance of such spectroscopic approaches: (i) Determination of the secondary structure and water accessibility of *Escherichia coli* outer membrane proteins led to reliable predictions of 3D structural models long before crystal structures were available (*12*). (ii) In the case of transport proteins such as lactose permease or Na^+,K^+-ATPase, important structural and dynamical elements for the transport process were found (*13*−*16*). (iii) Central steps in the proton translocation process of bacteriorhodopsin were elucidated, resolving structural changes of single amino acid residues (*17*). (iv) For channel proteins such as aquaporin or acetylcholine receptor, the structure of the membrane-spanning part was predicted (*18*−*20*).

In published reports, infrared spectroscopic investigations require typically milligrams of protein, which is slightly less than used for X-ray and NMR spectroscopy but still orders of magnitude too high to access most of the pharmacologically important mammalian receptor proteins, which are not available in these amounts.

Here we report on FTIR[1] spectroscopy with nanogram quantities of membrane proteins, which is 4−5 orders of magnitude less than used for conventional FTIR methods. Our novel approach is based on the formation of micrometer-sized, fully hydrated membrane protein samples on IR

† This work was financially supported by the Swiss National Science Foundation.

* Corresponding author: Tel +41-21-6933155; fax +41-21-6936190; e-mail horst.vogel@epfl.ch.

[1] Abbreviations: FTIR, Fourier transform infrared; H/D exchange, hydrogen/deuterium exchange; μFTIR, microscope Fourier transform infrared; 5-HT_3R, 5-hydroxytryptamine type 3 receptor; nAChR, nicotinic acetylcholine receptor.

10.1021/bi035113k CCC: $25.00
Published on Web 11/07/2003

transparent plates and their investigation by a microscope FTIR (μFTIR) spectrometer. We first examined the reliability of our method by determining the secondary structure of nAChR in native membranes isolated from *Torpedo californica*. For this prototypic ligand-gated ion channel , there are not only a number of FTIR studies reported in the literature (*21*−*23*) but also a 4 Å resolution 3D protein structure of the extracellular and transmembrane regions (*24*). We then proceeded to investigate 5-HT_3R, a ligand-gated ion channel protein that is presently available in purified form only in small quantities (*25*). Two different types of experiments were performed: (i) determination of the overall protein secondary structure and (ii) measurement of the spectral changes upon exchanging H_2O by D_2O to probe the secondary structure of the water-accessible parts of 5-HT_3R and nAChR in both cases for the first time. H/D exchange FTIR experiments were pioneered by de Jongh et al. (*26*) for water-soluble proteins but never applied to membrane proteins.

MATERIALS AND METHODS

Materials. CaF_2 plates (2 mm thick, 13 mm diameter) were from Korth; asolectin (soybean lipids) and all organic solvents were from Fluka. Nona(ethylene glycol) mono-*n*-dodecyl ether ($C_{12}E_9$) was from Anatrace, while all other lipids were from Avanti Polar Lipids. Aqueous solutions were made with 18 MΩ/cm deionized water (Nanopure, Barnstead Inc.) or with D_2O (99.8% purity, Dr. Glaser AG).

Receptor Preparations. Expression (*27*) and purification (*25*) of the 5-HT_3R protein containing a hexahistidine tag at the N-terminus are described elsewhere as indicated. nAChR-rich membranes, a gift from Professor F. Hucho (FU Berlin, Germany), have been produced as described elsewhere (*23*). nAChR was solubilized in detergent ($C_{12}E_9$) according to a previously published protocol (*28*). Reconstitution of 5-HT_3R into lipid bilayers was done as follows: Lipid vesicles were produced by dissolving 1 mg/mL asolectin in $CHCl_3$, followed by evaporation of the solvent. Subsequently, the lipid film was rehydrated with 1 mL of water and the lipid suspension was sonicated with a tip sonifier for 2 min. The vesicle suspension was mixed with detergent-solubilized 5-HT_3R at a lipid-to-protein ratio (w/w) of 5 and incubated for 2 h at 4 °C. Finally, $C_{12}E_9$ was removed by dialysis against deionized water by use of a slide-a-lyzer (3500 MW cutoff, Perstorp).

μFTIR. Infrared transmission spectra were obtained on an IRscope II infrared microscope connected to an IFS 28 infrared spectrometer (Bruker AG). If only one protein sample was investigated, we usually spread 5 μL of an aqueous protein solution (0.01 mg/mL) directly on a hydrophobic CaF_2 plate that was then transferred to a desiccator to evaporate excess water (5 min at 30 mbar by water aspiration), thus producing a 500 μm diameter hydrated protein film. One hundred cycles of 50 single-beam spectra, each at a nominal resolution of 1 cm^{-1}, were collected for both sample and reference by use of a computer-controlled xy-stage and then averaged. Residual gaseous as well as liquid water contributions were removed from the spectra by interactively subtracting absorbance spectra of gaseous and liquid water acquired previously. Final data were Fourier-transformed to 4 cm^{-1} frequency resolution by use of a triangular apodization function. The water content of a protein thin film was estimated by comparing the intensities of the water and the protein absorption bands at 3408 and 1656 cm^{-1}. The signal-to-noise ratio was calculated by taking the ratio between the maximal intensity of the amide I band and the intensity of the background between 1750 and 2000 cm^{-1}.

Overall Protein Secondary Structure. Protein secondary structure was evaluated by analyzing the amide I region between 1700 and 1500 cm^{-1} of protein samples in H_2O and in D_2O. Protein spectra corrected for atmospheric and liquid water were then subject to a resolution enhancement routine by maximum entropy/bayesian deconvolution using a Lorentzian peak shape with a full bandwidth at half-height (fwhh) of 20 cm^{-1} (Razortools/6, Spectrum Square). The amide I band of the deconvoluted spectrum was fitted as a sum of individual bands by a procedure established by Susi and Byler (*29*). Intensities, bandwidths, and frequencies of the individual bands of the deconvoluted spectra were used as starting values for fitting the nondeconvoluted spectra by a linear combination of Gaussian and Lorentzian bands.

Overall H/D Exchange Kinetics. A transmission cuvette was constructed that allowed purging the sample with a flow of D_2O-saturated nitrogen. During H/D exchange typically 50 interferograms from protein and from reference were measured. Spectral changes during H/D exchange were measured at time t as band areas $A_I(t)$ between 1700 and 1600 cm^{-1} for the amide I band and $A_{II}(t)$ between 1590 and 1503 cm^{-1} for the amide II band. To correct for any changes in total intensity of the spectra during the H/D exchange, intensity ratios $A_{II}(t)/A_I(t)$ were always considered. The fraction of nonexchanged amide bands at time t is

$$x(t) = A_{II}(t)/\omega A_I(t) \quad (1)$$

with $\omega = A_{II}(0)/A_I(0)$ of the fully hydrated protein before H/D exchange. Typically ω adopts values between 0.4 and 0.5.

H/D Exchange of Individual Secondary Structures. We followed a procedure developed by de Jongh et al. (*26*). To obtain the exchange kinetics for each of the four individual classes of secondary structures (α-helix, β-strand, β-turn, and nonregular structures), amplitudes at different frequencies of the amide I region were monitored during H/D exchange. First the isosbestic point of the amide I band for the H/D exchange of the nonregular structures was determined to be at 1652 cm^{-1} by analyzing the first 10 min of the exchange kinetics. At this frequency only α-helical exchange is obtained. Since the exchange kinetics at 1656 cm^{-1} reflects both α-helices and nonregular structures, the α-helical contribution of exchange kinetics has to be subtracted from the nonregular exchange kinetics in order to get the exchange kinetics of the latter. The contribution of the α-helical exchange at 1656 cm^{-1} is obtained by adjusting the slope of the exchange curve to zero between 100 and 1400 min. The exchange kinetics of β-strands was obtained by monitoring the amplitude at 1620 cm^{-1}. Exchange kinetics of β-turns was determined at 1675 cm^{-1}. At this frequency the contribution of the β-strand exchange kinetics has to be subtracted by using the method mentioned above.

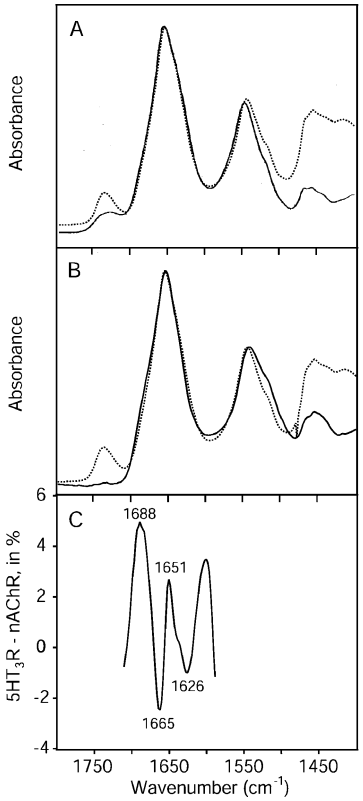

FIGURE 1: FTIR spectra of 5-HT_3R and nAChR. (A) Transmission IR spectrum of nAChR (solid line, taken from ref *23*) and μFTIR spectrum of nAChR (dashed line). (B) μFTIR spectra of detergent-solubilized 5-HT_3R recorded in H_2O (same as above μFTIR nAChR spectrum). The spectra are normalized with respect to the amide I band. Spectral contribution of liquid and atmospheric H_2O have been subtracted. (C) Percent difference between μFTIR spectra of detergent-solubilized 5-HT_3R and nAChR in native membranes recorded in H_2O.

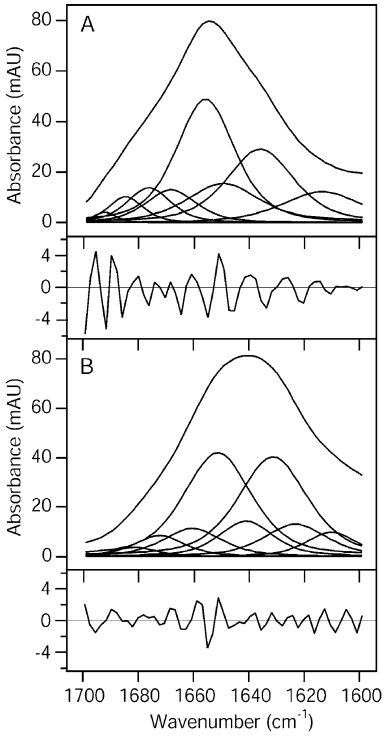

FIGURE 2: Deconvolution and fitting of the amide I bands. (A) The amide I band of detergent-solubilized 5-HT_3R in H_2O was fitted by a sum of Gaussian and Lorentzian bands. (B) Curve fitting the amide I′ band of detergent-solubilized 5-HT_3R in D_2O. This spectrum was obtained after deuteration of the sample used for recording the spectrum shown in panel A. Traces below the fits show the residuals in milliabsorbance units (mAU).

RESULTS

General Characteristics of FTIR Spectra of 5-HT_3R and nAChR. A μFTIR spectrum of a hydrated film of nAChR was superimposed on a conventional transmission spectrum of suspensions of nAChR membranes obtained either by Naumann et al. (*23*) or in our laboratory. The spectra almost perfectly overlap (Figure 1A). This demonstrates that the secondary structure of nAChR in a hydrated film is identical to that in the original membrane suspension and also that spectra obtained by conventional FTIR spectroscopy using tens of milligrams of protein and by μFTIR using 50 ng of protein are identical.

μFTIR spectra of detergent-solubilized 5-HT_3R and of nAChR in lipid membranes from different sample preparations were compared and showed high reproducibility. The difference between 5-HT_3R and nAChR amide I spectra (Figure 1C) deviates at no frequency more than 5%, corroborating the similarity of the structure of both proteins. The positive band at 1688 cm^{-1} is most probably due to side-chain absorption of Asn, Arg, and Gln which is higher for 5-HT_3R than for nAChR. The band at 1651 cm^{-1} indicates changes in the α-helix structures. The small negative bands at 1665 and 1626 cm^{-1} might correspond to a decrease in β-turns and β-strands, respectively. Considering that one receptor subunit comprises about 500 amino acids, the percent changes of the secondary structure correspond to about 5 (1626 cm^{-1}) to 10 (1651 and 1665 cm^{-1}) amino acids.

High signal-to-noise ratio (over 1000) FTIR spectra were obtained from minute amounts (50 ng) of receptor. This was achieved by confining hydrated protein samples to hydrophilic areas on an otherwise hydrophobic CaF_2 plate and measuring them with an infrared microscope repetitively between sample and reference, thus creating very stable recording conditions.

By comparing the intensities of H_2O (3408 cm^{-1}) and the amide I and II bands of receptor preparations, the weight ratio of water/protein was determined to be 1/2 or higher which is sufficient to preserve the functional integrity of the receptors (*30*, *31*).

Secondary Structure of 5-HT_3R and nAChR. Deconvolution of the amide I and I′ bands identified seven to eight bands for both 5-HT_3R and nAChR (Figure 2, Table 1). A band characteristic of α-helices appeared at 1658 cm^{-1} for nAChR and at 1656 cm^{-1} for 5-HT_3R. In D_2O the α-helix band is slightly shifted to 1653 cm^{-1} for both proteins. The band at 1642 cm^{-1} observed in deuterated samples of both 5-HT_3R and nAChR was assigned to nonregular structures (*9*). Other bands found near 1683, 1692, and below 1640 cm^{-1} were assigned to β-strands, while those found between 1682 and 1660 cm^{-1} were assigned to bendlike and turnlike structures.

The estimated secondary structure of 5-HT_3R consists of 36% α-helix, 33% β-strand, 15% β-turn, and 16% nonregular structures (Table 2). No significant differences were observed when 5-HT_3R was reconstituted in asolectin membranes, a

Table 1: Secondary Structure of 5-HT_3R and nAChR from Analysis of the Amide I and I′ Bands[a]

H_2O (5-HT_3R/nAChR)			D_2O (5-HT_3R/nAChR)		
position (cm^{-1})	abundance (%)	assignment	position (cm^{-1})	abundance (%)	assignment
1693/1690	4/4	β-strand	1682/1682	2/3	β-strand
1683/1682	5/5	β-strand	1673/1674	5/4	β-turn
1673/1675	9/5	β-turn	1663/1669	8/8	β-turn
1666/1668	7/6	β-turn	1653/1653	33/36	α-helix
1656/1658	36/35	α-helix	1642/1642	16/14	nonregular
1645/1644	18/20	nonregular	1632/1631	29/30	β-strand
1636/1632	21/25	β-strand	1623/1621	7/5	β-strand

[a] 5-HT_3R was solubilized in $C_{12}E_9$; nAChR was solubilized in native membranes. The amide I (H_2O) and the amide I′ (D_2O) bands were fitted by a linear combination of Gaussian and Lorentzian bands. Shown are the position (wavenumbers), abundance as a percentage of total, and secondary structure assignment of each decomposed band.

Table 2: Secondary Structure of Different Preparations of 5-HT_3R and nAChR Determined from Analysis of the Amide I and I′ Bands[a]

	secondary structure (%)			
	α-helix	β-strand	β-turn	nonregular
total 5-HT_3R[b]	36 ± 5	33 ± 7	15 ± 8	16 ± 7
total 5-HT_3R[c]	33 ± 4	37 ± 8	17 ± 6	13 ± 8
water-accessible 5-HT_3R[d]	14	16	26	14
total nAChR[b]	34 ± 6	37 ± 5	14 ± 5	15 ± 6
total nAChR[e]	37 ± 7	37 ± 4	12 ± 7	14 ± 5
water-accessible nAChR[f]	16	17	14	14

[a] Average of 4 measurements (2 in H_2O and 2 in D_2O). [b] Solubilized in $C_{12}E_9$ detergent. [c] Reconstituted in asolectin membranes. [d] Solubilized in $C_{12}E_9$ detergent, after 24 h of H/D exchange. Only one measurement. [e] Native membranes. [f] Native membranes, after 24 h of H/D exchange. Only one measurement.

lipid mixture that has been used for reconstitution of many membrane proteins (*32*).

μFTIR spectra of nAChR preparations in native membranes and solubilized in the detergent $C_{12}E_9$ were also subjected to curve fitting. Frequencies and intensities of the individually resolved bands and in turn estimated secondary structures correspond very well with those found for 5-HT_3R (Table 2).

H/D Exchange of 5-HT_3R and nAChR. The water accessibility of the proteins was investigated by measuring the H/D exchange of the amide bands of (i) 5-HT_3R solubilized in detergent and reconstituted in lipid membranes and (ii) nAChR in native membranes and solubilized in detergent. In all cases the kinetics of appearance of the amide II′ band can be described by a double-exponential function (Figures 3 and 4).

As a general result of a detailed analysis of the H/D exchange kinetics, summarized in Table 3, detergent-solubilized receptors exchange 4 (5-HT_3R) to 3 (nAChR) times faster than membrane-inserted ones.

Secondary structures of water-accessible parts of 5-HT_3R and nAChR can be resolved from the H/D exchange kinetics by the procedure of de Jongh et al. (*26*).

(*i*) *Detergent-Solubilized 5-HT_3R.* The time course of each of the IR-distinguishable secondary structure class was fitted by a biexponential function (Figure 5). Taking into account that 30% of the hydrogens are exchange-resistant, the intensity changes at particular frequencies yielded for the water-accessible part of 5-HT_3R 14% α-helix, 16% β-strand, 26% β-turn, and 14% nonregular structures.

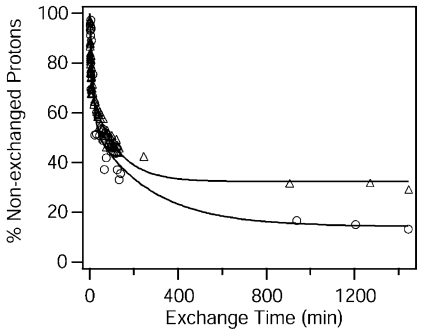

FIGURE 3: H/D exchange kinetics of different 5-HT_3R preparations by μFTIR. Measured are intensity ratios of amide II/amide I bands according to eq 1: (○) 5-HT_3R reconstituted in asolectin membranes; (△) 5-HT_3R solubilized in detergent $C_{12}E_9$. Exchange curves were fitted with a double-exponential function. Acquisition of the first 20 spectra was carried out accumulating 50 scans, followed by 5 spectra acquired every hour using 500 scans. The last spectrum was recorded accumulating 1000 scans.

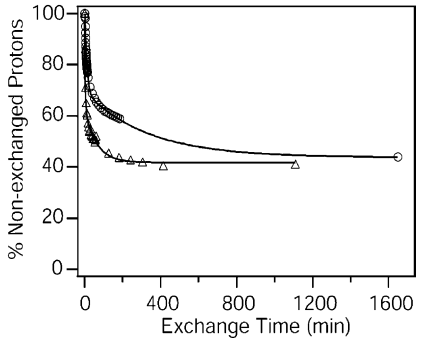

FIGURE 4: H/D exchange kinetics of different nAChR preparations: (○) native nAChR membranes; (△) detergent-solubilized nAChR. Exchange curves were fitted with a biexponential function. Recording conditions were as described for Figure 3.

Table 3: Kinetics of H/D Exchange of 5-HT_3R and nAChR[a]

	5-HT_3R		nAChR	
	in asolectin	in $C_{12}E_9$	in native membranes	in $C_{12}E_9$
A_1	38 ± 10	31 ± 2	24 ± 1	21 ± 2
τ_1 (min)	262 ± 130	119 ± 13	227 ± 20	64 ± 11
A_2	49 ± 9	37 ± 2	32 ± 1	37 ± 2
τ_2 (min)	17 ± 8	4 ± 1	6 ± 1	3 ± 1
A_∞	13 ± 4	32 ± 2	44 ± 1	42 ± 1

[a] Changes of the normalized amide I/amide II intensity ratios $x(t)$ were fitted by $x(t) = A_1 \exp(t/\tau_1) + A_2 \exp(t/\tau_2) + A_\infty$.

(*ii*) *nAChR in Native Membranes.* The H/D exchange kinetics of the four secondary structure classes (Figure 6 of Supporting Information) are similar to those of 5-HT_3R. The water-accessible part of nAChR comprises 16% α-helix, 17% β-strand, 14% β-turn, and 14% nonregular structures.

DISCUSSION

Secondary Structure of nAChR and 5-HT_3R. The secondary structures of 5-HT_3R and nAChR as determined from amide I band analysis are very similar, which is in agreement with their common features: (i) Both are members of the same ligand-gated ion channel family (*33*, *34*). (ii) They share common structural features: an extracellular N-terminal domain of about 220 amino acids, four predicted hydrophobic

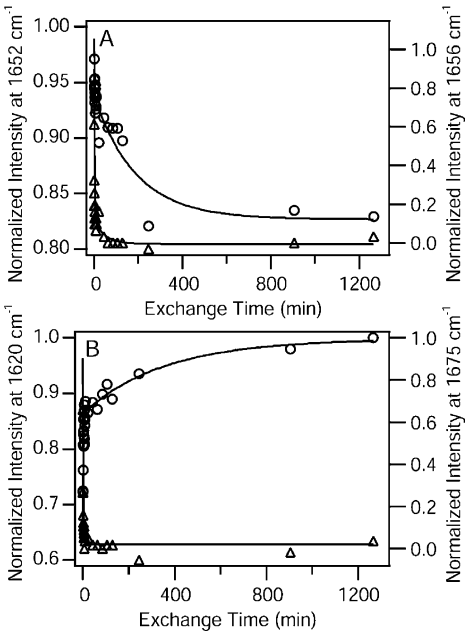

FIGURE 5: H/D exchange kinetics of individual secondary structure elements of detergent-solubilized 5-HT$_3$R. Band intensities were monitored at (A) 1652 cm^{-1} (α-helices, ○), 1656 cm^{-1} (nonregular structures, △), (B) 1620 cm^{-1} (β-strands, ○), or 1675 cm^{-1} (β-turns, △) and plotted as a function of exchange time to D_2O. Kinetic data fitted by a biexponential function yielded slow time constants in decreasing order: τ_1(helix) = 243 ± 50 min, τ_1(β-strand) = 190 ± 30 min, τ_1(nonregular) = 20 ± 5 min, and τ_1(β-turn) = 2 ± 2 min. The fast time constant τ_2 was between 1 and 2 min for all secondary structures.

transmembrane helices (*20*, *35*−*37*), a large hydrophilic cytoplasmic domain, and a very short extracellular carboxyl terminus. (iii) The extracellular N-terminal domains of both 5-HT$_3$R and nAChR are predicted to comprise mainly β-strands (*38*). The fewest data are available for the cytoplasmic part, which is predicted to consist of two amphipathic helices connected by a loop (*39*).

Taken together, the presented structural information yields a consensus secondary structure for both receptors of 31% α-helix, 33% β-strand, and 36% turn + nonregular features, which corresponds reasonably well with secondary structure derived from our infrared data for 5-HT$_3$R and for nAChR. The structural comparison between the two receptors performed in this paper is highly reliable because our results were obtained under strictly identical experimental conditions. This is important to note because secondary structures of ligand-gated ion channels reported from different laboratories vary considerably (see Table 4 in Supporting Information).

Nevertheless, the slight but reproducible differences between the FTIR spectra of 5-HT$_3$R and nAChR seen in Figure 1C also demonstrate that conformational differences in the order of 5−10 amino acids per receptor subunit are measurable. A detailed analysis of mutant receptor proteins might help in the future to localize the structural differences within the corresponding protein sequence.

Influence of Environment on Secondary Structure and H/D Exchange. Results obtained from membrane-integrated and detergent-solubilized nAChR and 5-HT$_3$R preparations are in line with previous studies showing that the secondary structure of membrane proteins is often similar in detergent and in membranes (*25*, *40*, *41*). Considering all the H/D exchange measurements performed with nAChR and 5-HT$_3$R, a clear pattern emerges that the fast and intermediate exchange time constants are higher for receptors incorporated in native membranes than in detergent.

H/D Exchange Kinetics of Secondary Structures. Exchange kinetics of the different secondary structure classes can be resolved, yielding in turn the average secondary structure of the water-accessible parts of the receptors. For both receptors there exists a population of amide hydrogens that are completely resistant to H/D exchange. It is reasonable to assume that this exchange-resistant part stems mainly from α-helices and β-strands, since β-turns and nonregular features are known to exchange very rapidly (*26*). H/D exchange experiments indicate that the exchange-resistant domains of the 5-HT$_3$R and the nAChR correspond to 14−16% α-helix and 16−17% β-strand of the overall secondary structure of 5-HT$_3$R and nAChR. As discussed earlier, the transmembrane helices of nAChR correspond to about 20% of the overall structure. It is tempting to assign the water-inaccessible α-helices to the transmembrane helices. Of the remaining water-accessible 20% α-helices, 15% might be shared among the extracellular N-terminal domain and the intracellular loop and 5% line the ion channel. The exchange-resistant 16% β-strands (out of total 35%) indicate high resistance to solvent accessibility, suggesting that they are located in the hydrophobic core of the N-terminal ligand binding domain (*38*).

CONCLUSIONS

From the large class of nAChR-like ligand-gated ion channels, until now extensive structural data exist only for nAChR. To our knowledge, we have here for the first time investigated, under strictly identical experimental conditions, prototypic ligand-gated ion channels of the Cys-loop family and have demonstrated that they adopt nearly identical secondary structures both for the overall protein and for the water-accessible parts. This strongly points toward the presumption that functionally closely related membrane proteins share also close structural relationships despite large amino acid sequence variability, in analogy to functional classes of water-soluble proteins such as the globin or antibody structures. The high signal-to-noise ratio spectra were obtained from minute amounts (50 ng)[2] of membrane proteins in the form of hydrated protein films investigated with an infrared microscope. Taking into consideration that typical expression quantities of recombinant membrane receptor proteins are between 10^5 and 10^6 receptors/cell, a 250 mL cell suspension culture, even at only 10% purification yield, will deliver sufficient membrane proteins to perform several FTIR experiments. This opens the possibility to access the structure and dynamics of many important mammalian receptor proteins. Obvious interesting applications are the investigation of the structure and dynamics of membrane proteins at different functional states (ligand−receptor and protein−protein interactions), comparing dif-

[2] The diameter of the hydrated receptor protein film (about 500 μm) on the CaF_2 support can be reduced by at least a factor of 3 to match the aperture of typical IR microscopes (about 150 μm) by use of a picoliter dispenser. Thus, it is a reasonable expectation to yield high-quality FTIR spectra from less than 5 ng of receptor proteins.

ferent mutant proteins to elucidate the functional role of distinct regions in the protein, as well as screening for optimal conditions during detergent solubilization, purification, reconstitution, and crystallization which is a prerequisite for successful structural determination at atomic resolution. The micrometer-sized samples used allow one to produce and investigate microarrays of receptor proteins.

ACKNOWLEDGMENT

We thank Professor Ferdinand Hucho for the nAChR membrane preparations.

SUPPORTING INFORMATION AVAILABLE

H/D exchange kinetics of the four secondary structure classes for nAChR in native membranes (Figure 6) and variation in secondary structures of ligand-gated ion channels reported from different laboratories (Table 4). This information is available free of charge via the Internet at http://pubs.acs.org.

REFERENCES

1. Berg, J., Tymoczko, J., and Stryer, L. (2002) *Biochemistry*, 5th ed., W. H. Freeman, New York.
2. Drews, J. (2000) *Science 287*, 1960−1964.
3. http://blanco.biomol.uci.edu/Membrane_Proteins_xtal.html (maintained by S. White, University of California, Irvine).
4. Fernandez, C., Adeishvili, K., and Wüthrich, K. (2001) *Proc. Natl. Acad. Sci. U.S.A. 98*, 2358−2363.
5. Sui, H. X., Han, B. G., Lee, J. K., Walian, P., and Jap, B. K. (2001) *Nature 414*, 872−878.
6. Locher, K. P., Lee, A. T., and Rees, D. C. (2002) *Science 296*, 1091−1098.
7. Kaback, H. R., Sahin-Toth, M., and Weinglass, A. B. (2001) *Nat. Rev. Mol. Cell. Biol. 2*, 610−620.
8. Abramson, J., Smirnova, I., Kasho, V., Verner, G., Kaback, H. R., and Iwata, S. (2003) *Science 301*, 610−615.
9. Goormaghtigh, E., Cabiaux, V., Ruysschaert, J. M. (1994) in *Subcellular Chemistry* (Hilderson, H. J., Ralston, G. B., Eds.) pp 329−450, Plenum Press, New York.
10. Tamm, L. K., and Tatulian, S. A. (1997) *Q. Rev. Biophys. 30*, 365−429.
11. Allin, C., Ahmadian, M. R., Wittinghofer, A., and Gerwert, K. (2001) *Proc. Natl. Acad. Sci. U.S.A. 98*, 7754−7759.
12. Vogel, H., and Jähnig, F. (1986) *J. Mol. Biol. 190*, 191−199.
13. Raussens, V., Ruysschaert, J. M., and Goormaghtigh, E. (1997) *J. Biol. Chem. 272*, 262−270.
14. Vogel, H., Wright, J. K., and Jähnig, F. (1985) *EMBO J. 4*, 3625−3631.
15. Le Coutre, J., Turk, E., Kaback, H. R., and Wright, E. M. (2002) *Biochemistry 41*, 8082−8086.
16. Le Coutre, J., Narasimhan, L. R., Patel, C. K. N., and Kaback, H. R. (1997) *Proc. Natl. Acad. Sci. U.S.A. 94*, 10167−10171.
17. Rammelsberg, R., Huhn, G., Lubben, M., and Gerwert, K. (1998) *Biochemistry 37*, 5001−5009.
18. Cabiaux, V., Oberg, K. A., Pancoska, P., Walz, T., Agre, P., and Engel, A. (1997) *Biophys. J. 73*, 406−417.
19. Görne-Tschelnokow, U., Strecker, A., Kaduk, C., Naumann, D., and Hucho, F. (1994) *EMBO J. 13*, 338−341.
20. Methot, N., Ritchie, B. D., Blanton, M. P., and Baenziger, J. E. (2001) *J. Biol. Chem. 276*, 23726−23732.
21. Butler, D. H., and McNamee, M. G. (1993) *Biochim. Biophys. Acta 1150*, 17−24.
22. Methot, N., McCarthy, M. P., and Baenziger, J. E. (1994) *Biochemistry 33*, 7709−7717.
23. Naumann, D., Schultz, C., Görne-Tschelnokow, U., and Hucho, F. (1993) *Biochemistry 32*, 3162−3168.
24. Miyazawa, A., Fujiyoshi, Y., and Unwin, N. (2003) *Nature 424*, 949−955.
25. Hovius, R., Tairi, A. P., Blasey, H., Bernard, A., Lundström, K., and Vogel, H. (1998) *J. Neurochem. 70*, 824−834.
26. de Jongh, H. H., Goormaghtigh, E., and Ruysschaert, J. M. (1997) *Biochemistry 36*, 13593−13602.
27. Pick, H., Preuss, A. K., Mayer, M., Wohland, T., Hovius, R., and Vogel, H. (2003) *Biochemistry 42*, 877−884.
28. Kröger, D., Hucho, F., and Vogel, H. (1999) *Anal. Chem. 71*, 3157−3165.
29. Susi, H., and Byler, D. M. (1986) *Methods Enzymol. 130*, 290−311.
30. Goormaghtigh, E., de Jongh, H. H., and Ruysschaert, J. M. (1996) *Appl. Spectrosc. 50*, 1519−1527.
31. Schinkel, J. E., Downer, N. W., and Rupley, J. A. (1985) *Biochemistry 24*, 352−366.
32. Gennis, R. B. (1989) *Biomembranes: Molecular Structure and Function*, Springer-Verlag, Heidelberg, Germany.
33. Reeves, D. C., and Lummis, S. C. (2002) *Mol. Membr. Biol. 19*, 11−26.
34. Karlin, A. (2002) *Nat. Rev. Neurosci. 3*, 102−114.
35. Changeux, J.-P. (1990) in *Fidia Research Foundation Neuroscience Award Lectures*, Raven Press Ltd., New York.
36. Williamson, P., Bonev, B., Barrantes, F., and Watts, A. (2000) *Biophys. J. 78*, 866.
37. Lugovskoy, A. A., Maslennikov, I. V., Utkin, Y. N., Tsetlin, V. I., Cohen, J. B., and Arseniev, A. S. (1998) *Eur. J. Biochem. 255*, 455−461.
38. Brejc, K., van Dijk, W. J., Klaassen, R. V., Schuurmans, M., van der Oost, J., Smit, A. B., and Sixma, T. K. (2001) *Nature 411*, 269−276.
39. Le Novère, N., Corringer, P. J., and Changeux, J. P. (1999) *Biophys. J. 76*, 2329−2345.
40. Dave, N., Troullier, A., Mus-Veteau, I., Dunach, M., Leblanc, G., and Padros, E. (2000) *Biophys. J. 79*, 747−755.
41. Abbott, G. W., Bloemendal, M., VanStokkum, I. H. M., Mercer, E. A. J., Miller, R. T., Sewing, S., Wolters, M., Pongs, O., and Srai, S. K. S. (1997) *Biochim. Biophys. Acta−Protein Struct. Mol. Enzymol. 1341*, 71−78.

BI035113K